

Phase diagram of helicoids in Chiral Liquid Crystals

G. De Matteis †*§, L. Martina †‡, C. Naya‡, V. Turco †‡

* IISS "V. Lilla", MIUR, Francavilla Fontana (BR) Italy

†Dipartimento di Matematica e Fisica, Università del Salento

‡INFN, Sezione di Lecce, Via per Arnesano, C.P. 193 I-73100 Lecce, Italy

§GNFM-INDAM, Città Universitaria - P.le Aldo Moro 5, C.P. 00185 Roma, Italy

(Dated: February 19, 2022)

Cholesteric Liquid Crystals (CLCs), in presence of an external uniform electric field and confined between two parallel planes with strong homeotropic anchoring conditions, are found to admit different types of helicoidal solutions with disclinations. Analytical and numerical analysis are performed in order to characterise their properties. In particular, we produce a phase transition diagram from the nematic state to the helicoids in terms of the chirality and the strength of the electric field.

Introduction – New static chiral states are found in Cholesteric Liquid Crystals (CLCs) which, in presence of an external uniform electric/magnetic field, are frustrated by imposing plane parallel boundary conditions to the Frank - Oseen free energy with strong homeotropic anchoring [1–3]. These configurations are similar to cholesteric fingers (helicoids) with defects of disclination type [4, 5]. The model is described by the elliptic Sine-Gordon equation on the strip with discontinuous boundary data. These states are stabilised both by topological and non-topological conservation laws[6].

In this letter, we classify and describe these configurations by analytical and numerical solutions. In particular, we discuss a new type of solutions called 2π -helicoids, where the director field $\mathbf{n}(\mathbf{r})$ rotates by 2π over the strip. All these solutions contain disclination type singularities; accordingly, the evaluation of the static free energy leads to the introduction of a phenomenological cut off, which, in turn, determines a critical parameter for the transition to the nematic uniform state.

In addition to the 2π -helicoids, we also find π -helicoids, where the director $\mathbf{n}(\mathbf{r})$ only performs a single twist over the strip. Transitions from the uniform nematic state to 2π - and π -helicoids are represented in the phase space of the spontaneous chiral twist and electric strengths.

The model – We consider a static CLC layer, confined in between two identical planar surfaces placed at $z = \pm \frac{L}{2}$, and extending to infinity in the orthogonal directions (x, y) in a suitable cartesian reference system (O, x, y, z) , with orthonormal basis vectors $\mathbf{x}, \mathbf{y}, \mathbf{z}$. The system is described by the uni-modular director field $\mathbf{n}(\mathbf{r}) = (\sin \theta(\mathbf{r}) \cos \phi(\mathbf{r}), \sin \theta(\mathbf{r}) \sin \phi(\mathbf{r}), \cos \theta(\mathbf{r})) \in \mathbb{RP}^2$, due to the Z_2 symmetry of the microscopic model [7], and governed by the Frank-Oseen free energy density

$$\begin{aligned} \mathcal{E}_{FO} = & \frac{K_1}{2} (\nabla \cdot \mathbf{n})^2 + \frac{K_2}{2} (\mathbf{n} \cdot \nabla \times \mathbf{n} - q_0)^2 \\ & + \frac{K_3}{2} (\mathbf{n} \times \nabla \times \mathbf{n})^2 + \frac{(K_2 + K_4)}{2} \nabla \cdot [(\mathbf{n} \cdot \nabla) \mathbf{n} \\ & - (\nabla \cdot \mathbf{n}) \mathbf{n}] - \frac{\varepsilon}{2} (\mathbf{n} \cdot \mathbf{E})^2, \end{aligned} \quad (1)$$

where q_0 is the spontaneous chirality constant of the cholesteric phase, while the positive reals K_i denote the splay, twist, bend and saddle-splay Frank elastic constants, respectively, for which we use the simplifying one constant approximation $K = K_1 = K_2 = K_3, \quad K_4 = 0$. The last term represents the energy density interaction with an external static electric field $\mathbf{E} = E \mathbf{z}$, which is assumed to be uniform.

At the bounding surfaces, we impose strong homeotropic anchoring conditions, *i.e.* $\mathbf{n}(x, y, z = \pm \frac{L}{2}) = \mathbf{z}$.

Both \mathbf{E} and the confinement break the general rotational and translational symmetry along the \mathbf{z} direction of the fundamental cholesteric helices, *i.e.* $\mathbf{n}(\mathbf{r}) = (0, \sin q_0 x, \cos q_0 x)$. Hence, cholesteric helices are deformed, possibly leading to extended structures called helicoids, or to localized cholesteric bubble domains, called spherulites, which have been considered in [8, 9].

The special symmetry reduction (constant $\phi = -\pi/2$ and y invariance)

$$\mathbf{n}(\mathbf{r}) = (0, -\sin \theta(x, z), \cos \theta(x, z)), \quad (2)$$

for the director field leads to the cholesteric finger phase with its axis along the \mathbf{x} direction and it simplifies the Frank-Oseen energy (1) to

$$\begin{aligned} E_{FO-2d} = & \frac{K}{2} \int_{-\frac{L}{2}}^{\frac{L}{2}} dz \int_{-\infty}^{\infty} dx \left[(\partial_x \theta(x, z))^2 + (\partial_z \theta(x, z))^2 \right. \\ & \left. + 2q_0 \partial_x \theta(x, z) + \frac{\varepsilon E^2}{K} \sin^2 \theta(x, z) \right]. \end{aligned} \quad (3)$$

The corresponding equilibrium equation is the elliptic sine-Gordon,

$$\partial_x^2 \Theta + \partial_z^2 \Theta = \Lambda^2 \sin \Theta, \quad \Theta = 2\theta, \quad \Lambda = \sqrt{\frac{\varepsilon}{K}} E. \quad (4)$$

The solutions in the plane for the equation (4) are well known in the literature [10], but here we are dealing with different boundary conditions. Our reduction

is the more natural extension of the problem considered in [11] and studied also in [12] in a linear setting with no external field. Here we study the nonlinear problem. Strong homeotropic anchoring conditions require $\Theta(x, \pm \frac{L}{2}) = 2k\pi$, for $k \in \mathbb{Z}$, and $\Theta(x, \pm \frac{L}{2}) = -2k'\pi$ for negative and positive x respectively. Thus, any non constant solution must have at least a jump singularity on the boundaries.

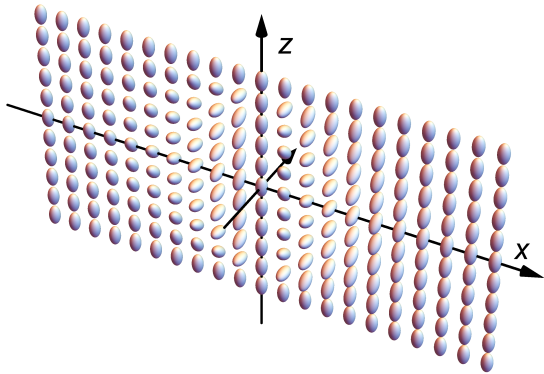


FIG. 1. Distribution of $\mathbf{n}(\mathbf{r})$ for the 2π -helicoid, given in (9) for $n = 0$. The picture shows a cross section of the configuration at $y = 0$.

2π - helicoids – A simple ansatz embodying the above requirements corresponds to solutions depending separately on the x and z variables [14]. Thus, we assume

$$\Theta = 4 \arctan [X(x) Z(z)]. \quad (5)$$

Plugging this expression into (4) yields a 2-parameter family of separated ODEs, namely,

$$X'' = 2aX^3 + (\Lambda^2 - d) X, \quad (6)$$

$$\frac{Z''}{Z} = -d - \frac{2a}{Z^2} + 2 \left(\frac{Z'}{Z} \right)^2, \quad (7)$$

where a and d are arbitrary integration constants. Integration of (6) can be performed by standard methods in terms of Jacobi elliptic functions.

The step-like conditions on the boundaries force to have $Z(\pm \frac{L}{2}) = 0$ and to look for functions $X(x)$ monotonic and unbounded, also at some finite point. Then, one obtains

$$X(x) = \pm \sqrt{\frac{\Lambda^2 - d}{a}} \operatorname{csch} \left(\sqrt{\Lambda^2 - d} x \right), \quad (8)$$

where $a > 0$ and $\Lambda^2 > d$.

As for $Z(z)$, the compatibility of the equation (7) with the sine-Gordon (4) and the above boundary conditions, set $d = -\frac{\pi^2}{L^2}$, in order to have real θ with the semi-period of the corresponding $Z(z)$ exactly equal to the thickness L of the sample. Thus, we are led to the general expression

$$\theta_n = 2 \arctan \left[\frac{c_n \ell}{\pi(1+2n)} \frac{\cos \left(\frac{\pi(1+2n)z}{L} \right)}{\sinh \left(c_n \ell \frac{x}{L} \right)} \right] - \pi \operatorname{sign} [x], \quad (9)$$

for $n \in \mathbb{N}$, and where the effective scale $\ell = \Lambda L$ and the modal factor $c_n = \left[1 + \frac{(1+2n)^2 \pi^2}{l^2} \right]^{\frac{1}{2}}$ have been introduced. The asymptotic behaviour of this family of solutions is $\theta \xrightarrow{x \rightarrow \pm \infty} \mp \pi$, that is, the director field $\mathbf{n}(\mathbf{r})$ rotates by 2π over the strip, as depicted in Fig. 1.

We first observe that the solution only depends on the structural parameters L and Λ . Second, there exists an entire spectrum of excitations indexed by $n \geq 0$. Since for $n > 0$ solutions are discontinuous at $x = 0$, the most physically meaningful solution corresponds to $\theta_0(x, z)$ (Fig. 1), which is continuous and differentiable at all points of the strip but the special points $(x = 0, z = \pm \frac{L}{2})$. Here it exhibits a discontinuity of 2π , indicating the presence of a disclination along the \mathbf{y} direction.

Whilst the dependency on z is determined uniquely by L , on the x variable the typical scale is $\Lambda^{-1} \left(1 + \frac{\pi^2}{\ell^2} \right)^{-\frac{1}{2}}$, which comes from the tendency of the external electric field to align the molecules along its direction, further enhanced by the anchoring of the bounding surfaces. We also notice that solution (9) can be obtained by applying the nonlinear Bianchi's superposition formula [13] for two 1-kink solutions of the elliptic sine-Gordon, with parameters β_1 and β_2 , respectively. In the present case the Bäcklund transformations are compatible with the imposed boundary conditions, although some restrictions on the parameters have to be introduced. Specifically, the two 1-kink solutions must have opposite phase and $\beta_1 = \frac{1}{\beta_2} = c_n + \sqrt{c_n^2 - 1}$. This result suggests that multiple 2π -helicoid solutions may be built up by finite methods.

Finally, let us observe that since the total change of θ is 2π , we can distinguish two regions where the director rapidly passes through $\frac{\pi}{2}$, sandwiched by three different regions in which the liquid crystal is close to the uniform state. Around the disclination, θ_0 has a conformally invariant behaviour which, in cylindrical coordinates $x = \rho \cos t$, $z = -\frac{L}{2} + \rho \sin t$, can be expressed as a series with respect to ρ , namely,

$$\theta_0 = -\operatorname{sign} [\cos t] \pi + 2t - \frac{\sin(2t) (\ell^2 \cos^2 t + \pi^2)}{6} \left(\frac{\rho}{L} \right)^2 + O \left(\left(\frac{\rho}{L} \right)^4 \right), \quad 0 \leq t \leq \pi. \quad (10)$$

Thus, θ_0 is almost independent of the distance ρ from the disclination. The corresponding singularity in the energy signals a loss of order, and therefore, physically, in the vicinity of the dislocation, the liquid crystal is melted from the ordered to the disordered isotropic phase. To avoid the singularity, we single out a small semi-disk, of radius $a \ll \frac{L}{2}$, around the disclination and replace it

with a region in the isotropic phase, where it is common practice to uniformly impose an energy density cut-off $\mathcal{E}_{max} \approx \frac{K}{a^2}$ with $a \approx 10^{-2} - 10^{-3}L$ [12].

By using analytical solution (9), we can write down an expression for the difference of energy with respect to the nematic phase in the limit of small a , which, up to second order, reads

$$\Delta E_{2\pi} = \frac{K}{3} \left[24G + 10a^2\Lambda^2 + 12\sqrt{\pi^2 + \Lambda^2 L^2} + 3a q_0 \log(16) - 2\pi \left(6 - 3a q_0 + 3Lq_0 + 2a^2\Lambda^2 + 6 \log\left(\frac{a}{2L}\right) + 3 \log\left(\Lambda^2 L^2 + 2\pi(\pi + \sqrt{\pi^2 + \Lambda^2 L^2})\right) \right) \right], \quad (11)$$

where G is the Catalan constant.

At thermal equilibrium, stable 2π -helicoids may exist if $\Delta E_{2\pi} < 0$; from the latter condition, one can infer a critical transition value for the chiral twist parameter as a function of the external field Λ . Notice that due to the presence of the external field, expansion (11) for small a holds as far as Λ is not very high, which is true in the

range of interest. By neglecting the a^2 contributions in (11) and introducing the cut-off energy, we arrive at

$$\Delta E_{2\pi} = 2KL(q_H - q_0) \left(\pi - \frac{1}{L} \sqrt{\frac{K}{\mathcal{E}_{max}}} (\pi + \log(4)) \right), \quad (12)$$

with

$$q_H = \frac{4G - 2\pi + 2\sqrt{\pi^2 + \Lambda^2 L^2} + \pi \log\left(4L^2 \frac{\mathcal{E}_{max}}{K}\right) - \pi \log\left(\Lambda^2 L^2 + 2\pi(\pi + \sqrt{\pi^2 + \Lambda^2 L^2})\right)}{L \left(\pi - \frac{1}{L} \sqrt{\frac{K}{\mathcal{E}_{max}}} (\pi + \log(4)) \right)}, \quad (13)$$

the critical chiral twist. Since the disclination radius has an important effect in locating the phase transition, q_H might be used to estimate the effective size of the defects appearing in real liquid crystal samples.

π -helicoids – In a “more elementary” class of helicoids the director $\mathbf{n}(\mathbf{r})$ twists only once, when going from the vacuum state $\theta = \pi$ at $x \rightarrow -\infty$, to the nearest \mathbb{Z}_2 equivalent one, namely $\theta = 0$ for $x \rightarrow +\infty$. Moreover, because of the homeotropic anchoring, the boundary conditions on the confining surfaces will be

$$\theta\left(x, z = \pm \frac{L}{2}\right) = \begin{cases} \pi & x < 0 \\ 0 & x > 0 \end{cases}. \quad (14)$$

Then, in such a kind of solutions, which we call π -helicoids, a couple of disclinations appear, parallel to the y axis.

The analysis of the full nonlinear boundary value problem (4) and (14) is quite involved and one might tackle it by starting from the methods developed in [15]. However, we managed to solve only the linear approximated version, which surely holds in the asymptotic regions $x \rightarrow \pm\infty$, by resorting to the techniques as in [16]. Thus, by also exploiting the discrete symmetry property of (4)

$$\theta(x, z) = \pi - \theta(-x, z), \quad (15)$$

one ends up with the pair of Helmholtz boundary value problems

$$\partial_x^2 \theta_+ + \partial_z^2 \theta_+ = \Lambda^2 \theta_+ \quad \forall x > 0, \quad (16a)$$

$$\theta_+\left(x, z = \pm \frac{L}{2}\right) = 0, \quad \theta_+(x = 0^+, z) = \frac{\pi}{2} \quad \forall |z| < \frac{L}{2},$$

$$\partial_x^2 \theta_- + \partial_z^2 \theta_- = \Lambda^2 (\theta_- - \pi) \quad \forall x < 0, \quad (16b)$$

$$\theta_-\left(x, z = \pm \frac{L}{2}\right) = \pi, \quad \theta_-(x = 0^-, z) = \frac{\pi}{2} \quad \forall |z| < \frac{L}{2}.$$

Therefore, from (15) θ_- can be obtained from θ_+ and vice versa.

In principle, this system could be solved by standard methods, however, the presence of the singularities at $(0, \pm \frac{L}{2})$ requires to adopt the method described in [16] on the semi-strip. By introducing the analytic dispersion functions on the punctured complex plane $\mathbb{C}_\lambda / \{0\}$

$$\Omega(\lambda) = \frac{i\Lambda}{2} \left(\frac{1}{\lambda} - \lambda \right), \quad \omega(\lambda) = \frac{\Lambda}{2} \left(\frac{1}{\lambda} + \lambda \right) \quad (17)$$

and the amplitudes in the \mathbb{C}_λ plane

$$G_1(\lambda) = \frac{i\pi}{4} \frac{1 - \lambda^2 e^{\omega(\lambda)L} - 1}{1 + \lambda^2 e^{\omega(\lambda)L} + 1}, \quad (18)$$

$$G_2(\lambda) = \frac{i\pi}{4} \frac{1-\lambda^2}{1+\lambda^2} \left(1 - e^{-\omega(\lambda)L}\right), \quad (19)$$

encoding the information about the boundary data, we are led to the integral representation for $\theta_+(x, z)$

$$\theta_+(x, z) = \frac{-1}{\pi} \left[\int_{-\infty}^0 e^{\Omega(\lambda)x + \omega(\lambda)(z + \frac{L}{2})} G_1(\lambda) \frac{d\lambda}{\lambda} + \int_{\infty}^0 e^{\Omega(\lambda)x + \omega(\lambda)(z - \frac{L}{2})} G_1(\lambda) \frac{d\lambda}{\lambda} - \int_{-i\infty}^0 e^{\Omega(\lambda)x + \omega(\lambda)(z + \frac{L}{2})} G_2(\lambda) \frac{d\lambda}{\lambda} \right]. \quad (20)$$

It is straightforward to prove that (20) satisfies the Helmholtz boundary value problem (16a), by looking at the analytic properties of the integrands in the lower half-plane \mathbb{C}_λ while suitably deforming the integration contour. Here, the function $G_1(\lambda)$ has the poles ($\ell = \Lambda L$)

$$P_G = \left\{ -i \left[\sqrt{\ell^2 + (2n+1)^2 \pi^2} - \pi(2n+1) \right] / L \right\}_{n \in \mathbb{Z}}. \quad (21)$$

Their residues lead to the series representation

$$\theta_+(x, z) = 2 \sum_{k=0}^{+\infty} \frac{(-1)^k}{2k+1} e^{-\frac{x \sqrt{\pi^2(2k+1)^2 + \ell^2}}{L}} \cos\left(\frac{\pi(2k+1)z}{L}\right), \quad (22)$$

which cannot be cast in a factorised form as in (9). Using expression (15) one can continuously complete the solution also for $x < 0$, except at the points $(0, z = \pm \frac{L}{2})$. The exponential decaying in x has the characteristic length $\Delta x \approx \frac{2L}{\sqrt{\ell^2 + \pi^2}}$. However, close to $x = 0$ the linear approximation of the sine-Gordon might be unsatisfactory. In addition, as $x \rightarrow 0$, (22) tends to the Fourier expansion of the pulse function of amplitude $\frac{\pi}{2}$, implying all well known convergence problems at the discontinuity points. Moreover, the partial derivative $\partial_x \theta(x \rightarrow 0^\pm, z)$ is not continuous in z , whereas $\partial_z \theta(x \rightarrow 0^\pm, z) = 0$. So the differentiability of θ on the segment $(x = 0, |z| < L/2)$ is lost.

In Fig. 2, $\mathbf{n}(x, z)$ is represented by using the formula (22) up to $k = 10$. At $(0, z = \pm \frac{L}{2})$ an overlap of directional ellipsoids occurs, thus giving rise to disclinations extended in the orthogonal direction y . However, the actual configuration is sensible to the involved parameters, which control also how good the linear approximation is. To have more insight in the π -helicoids, a numerical boundary value problem solver has been implemented for the full nonlinear problem. The agreement between (22) and the numerical solution improves as Λ increases. This stems from the vanishing of the characteristic length Δx . *Phase transition diagram* – In order to assess the relative stability of the solutions we have found above, *i.e.*, π - and 2π -helicoids, we need now to perform an energy analysis and to compare the solutions also with the uniform nematic configurations to see which one is energetically favoured in terms of the physical parameters involved, namely q_0 and Λ . Recalling that the chiral strength q_0 is

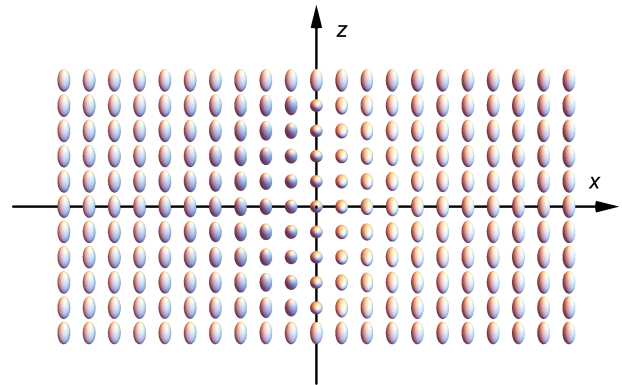


FIG. 2. Distribution of the $\mathbf{n}(x, z)$ field for the π -helicoid.

a function of the temperature (linear under certain conditions), one could interpret the phase diagram as the result of thermal-electric competitive effects in the formation of the helicoids. When the energy of both solutions is greater than zero, the homeotropic nematic phase is the favoured one. It is important to note that the transitions between the three different configurations occur along two different curves (see Fig. 3). There are two different thresholds in chirality strength, for fixed electric field, also depending on the disclination size a/L . In Fig. 3, we have set $a/L = 10^{-2}$, although for smaller values of a/L the shape of the diagram does not change. In particular, the curve between the nematic and π -helicoid phases should be the analogous of the straight line $\Lambda_0 = \frac{\pi|q_0|}{2}$ in the bulk model [17]. Deviations from such a behaviour are related to the anchoring, possibly leading to significant variations in the value of the critical electric field. Moreover, in [12] it was found a semi-empirical coexistence curve between the homeotropic and the cholesteric phase, providing the critical electric field $\Lambda_c L$ in terms of the cholesteric twist $q_0 L$. Using the present notation, such a relation reads

$$\Lambda_c L = \sqrt{\frac{2\gamma^2 q_0 L \left(q_0 L - \frac{2}{\gamma} \right)}{1 - \frac{(1 - e^{-\gamma q_0 L})}{\gamma q_0 L}}}, \quad (23)$$

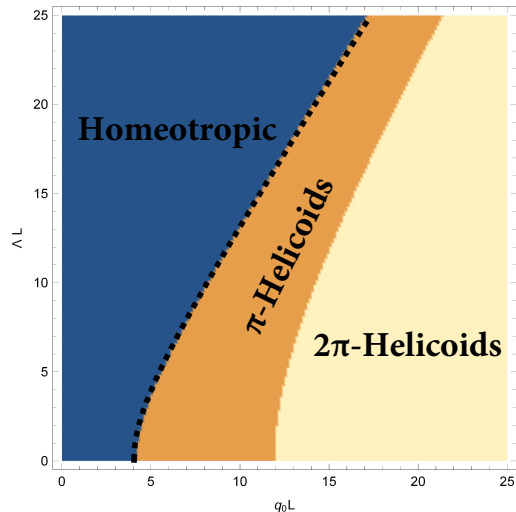


FIG. 3. Phase diagram in the plane $Lq_0, L\Lambda$, representing the nematic (blue), π -helicoid (orange) and 2π -helicoid (ochre) phases. The dashed black line corresponds to the best fit to (23).

with $\gamma = K_2/K$ and

$$qL = -\frac{1}{\gamma} W_{-1} \left(-\frac{\gamma}{2c} e^{-1-q_0 L \gamma} \right), \quad (24)$$

where W_k is the k -th branch of the Lambert W function [18]. A fitting procedure to our numerical data leads to $\gamma = 1.054$, in excellent agreement with our assumed one constant approximation (*i.e.* $\gamma = 1$). The corresponding best fit curve is displayed in Fig. 3 (black dashed line).

Conclusions – Summarizing, we have analytically found 2π -helicoids which, in our knowledge, are novel configurations in bounded CLC with homeotropic anchoring, allowed by the nonlinearity arising from the presence of an external field. Analogously, we studied a different type of helicoids, the π ones. If the former configuration can be derived in a closed form, for instance by the Bäcklund transformations, for the latter we have obtained approximated expressions and numerical solutions. Both classes of configurations are characterised by the presence of disclinations, located at the boundaries. The disclinations imply energy density divergences, which may be overcome by introducing a phenomenological energy cut off, corresponding to excluded regions of melted crystal.

Numerically, we provided a phase diagram in the parameters $q_0 L$ and $L\Lambda$, which established the energetically

favoured configurations among them and the uniform nematic phase and the corresponding transitions. In particular, for fixed value of the external field, we found the sequence uniform-to- π -to- 2π -helicoids as the value of the chirality increases, as expected. The next step to be taken might be the study of the existence of lattices of helicoids, their interactions and the corresponding phase diagram.

Acknowledgments. CN is supported by the INFN grant 19292/2017 *Integrable Models and Their Applications to Classical and Quantum Problems*. LM has been partly supported by INFN IS-CSN4 *Mathematical Methods of Nonlinear Physics*.

-
- [1] R. D. Kamien and J. V. Selinger, *J. Phys. Condens. Matter* **13**, R1 (2001).
 - [2] P. Oswald and P. Pieranski, *Nematic and Cholesteric Liquid Crystals: Concepts and Physical Properties Illustrated by Experiments* (CRC Press, 2005).
 - [3] I. I. Smalyukh, B. I. Senyuk, P. Palffy-Muhoray, O. D. Lavrentovich, H. Huang, E. C. Gartland, V. H. Bodnar, T. Kosa, and B. Taheri, *Phys. Rev. E* **72**, 061707 (2005).
 - [4] J. Baudry, S. Pirkel, and P. Oswald, *Phys. Rev. E* **57**, 3038 (1998).
 - [5] P. Oswald and A. Dequidt, *Phys. Rev. E* **77**, 051706 (2008)
 - [6] J.-i. Fukuda and S. Žumer, *Phys. Rev. Lett.* **104**, 017801 (2010).
 - [7] P. De Gennes and J. Prost, *The physics of liquid crystals*, (Clarendon Press, Oxford, 1993).
 - [8] G. De Matteis, L. Martina, V. Turco, *Theor. Math. Phys.* **196**, 1150 - 1163,(2018).
 - [9] G. De Matteis, D. Delle Side, L. Martina, V. Turco, *Phys. Rev. E* **98**, 042702 (2018).
 - [10] Borisov, A , Kiselev, V., *Inverse Problems* **5**, 959-982 (1999).
 - [11] S. Afghah, J. V. Selinger, *Phys. Rev. E* **96** 012708 (2017).
 - [12] J. C. Lee, D. W. Allender, V. D. Neff, *Mol. Cryst. Liq. Cryst.* **210**, 11-20 (1992).
 - [13] Rogers C. and . Schief W. K. , *Bäcklund and Darboux Transformations*, (Cambridge Univ. Press, Cambridge, 2002), pag. 30.
 - [14] S.V. Burylov, A.N. Zakhlevnykh, *Eur. Phys. J. E* **39** , 65 (2016).
 - [15] Fokas, A. S. and Lenells, J. and Pelloni, B, *J. Nonlin. Sci.* **23**, 241–282 (2013).
 - [16] Y. Antipov and A.S. Fokas, *Math. Proc. Camb. Phil Soc.* **138**, 339-365 (2005).
 - [17] P. J. Kedney, I. W. Stewart, *Lett. Math. Phys* **31**, 261-269 (1994).
 - [18] DLMF - NIST : <https://dlmf.nist.gov/4.13>